# Introducing a simple convex hull method to calibrate diffusion coefficients in Lagrangian particle models

Yang Song[a*], Ayumi Fujisaki-Manome[a,b], Christopher H. Barker[c], Amy MacFadyen[c], Dan Titze[d], James Kessler[d], Jia Wang[d]

[a] Cooperative Institute for Great Lakes Research, School for Environment and Sustainability, University of Michigan, Ann Arbor, MI 48109, United States

[b] Climate & Space Sciences and Engineering, University of Michigan, Ann Arbor, MI 48109, United States

[c] NOAA Office of Response and Restoration, Seattle, WA 98115, United States

[d] NOAA Great Lakes Environmental Research Laboratory, Ann Arbor, MI 48108, United States

[*]Corresponding author

*Email address*: songyangscu@hotmail.com; soyang@umich.edu (Y. Song).

## Abstract

Calibrating Lagrangian particle models (LPMs) is crucial for simulating oil spill trajectories, enabling emergency responses, and mitigating harmful effects on the environment. However, there is a lack of rigorous observation data on oil spill events, especially in water bodies with no serious spills but perceived increasing risk, hampering LPM application. This study utilized trajectory data from three drifters in Lake Erie, collected in 2016, 2018, and 2019. We then proposed a simple and efficient convex hull method to identify the smallest envelope of the simulated particle cloud, covering all drifter trajectories while simultaneously controlling over-diffusion. This approach was employed to calibrate the General NOAA Operational Modeling Environment oil spill model (an LPM) and determine optimal diffusion coefficients. Based on 362 one-day-long drifter trajectory simulation cases, the recommended diffusion coefficient for particle trajectory simulation in Lake Erie was determined to be 14 $m^2$ $s^{-1}$. The calibrated model demonstrated the ability to effectively capture the movement direction of drifters and control the discrepancy between simulated and observed trajectories. Meanwhile, it underestimated drifter travel distances due to errors in input currents, the primary force driving drifter movement. These results promote LPM application for particle trajectory simulations.

## Keywords

Lagrangian model; Diffusion process; Oil spill transport; Drifter trajectory; Convex hull; Performance metrics.

## 1. Introduction

As global energy consumption, population, and economic development continue to grow, the exploitation, trade, and transportation of oil are on the rise (Albeldawi, 2023; Chen et al., 2019). Consequently, there is an increasingly high risk of oil spill incidents, including ship collisions, wrecks, pipeline leaks, and illegal dumping (Balogun et al., 2021; Cakir et al., 2021; Li et al., 2016). These oil spills pose significant threats and damage to the aquatic environment and ecology, can lead to the death of fish and birds, as well as impacting socioeconomic resources such as fisheries and tourism (Bhattacharjee and Dutta, 2022). Moreover, the health of cleanup workers and residents exposed to the contaminated areas is also at severe risk (Johnston et al., 2019). Efficient emergency response to oil spill accidents and the mitigation of their harmful effects require the use of Lagrangian particle models (LPMs) to predict oil spill trajectories, providing crucial information to emergency personnel (Barker et al., 2020; Keramea et al., 2021). Therefore, the calibration of LPMs is paramount for their effective use in simulating oil spill trajectories. These steps significantly influence the accuracy and efficiency of emergency response efforts.

Previous studies have employed various LPMs to simulate oil spill trajectories, including well-known models like the General NOAA Operational Modeling Environment (GNOME) oil spill model, the Oil Spill Contingency and Response model (OSCAR), and the OpenOil model, to simulate and analyze oil spill transport and spreading (Balogun et al., 2021; Dagestad et al., 2018; Dong et al., 2019; Keramea et al., 2021; Nordam et al., 2019; Xu et al., 2012). Several calibration methods have been examined for these LPMs to optimize coefficients used in specific applications. For example, researchers calibrated the current, wind, and wave coefficients in an LPM using 13 drifting buoys deployed in the Bay of Biscay during the *Prestige* oil spill accident (Abascal et al., 2009). A previous study based on satellite images employed the mean center position and the mean major direction as evaluation metrics to minimize the difference between simulated and observed trajectories, thereby improving calibration to obtain the optimal combination of coefficients used in an LPM (Tian et al., 2017). Furthermore, researchers recently found that the Kullback-Leibler divergence-based calibration method, which utilizes satellite images, could enhance the effectiveness of spill trajectory predictions from an LPM compared to distance-based calibration methods (Yang et al., 2023). Collectively, previous studies recognized the need for precise calibration in spill trajectory modeling and proposed intricate mathematical methods to determine the optimal coefficient combination (De Dominicis et al., 2013; Goeury et al., 2014; Guo et al., 2018; Ivanov et al., 2021; Jiang et al., 2021).

However, many of these calibration methods depended on opportunistic satellite images that were available during a limited number of actual spill events, and were predominantly focused on coastal and marine environments (Dearden et al., 2022; Tian et al., 2017; Yang et al., 2023). Research on using drifter or buoy data for proactively calibrating LPMs in advance of spill events is scarce, particularly in freshwater environments where applied experience with LPMs and reliable parameter settings are severely lacking. In addition, previous calibration in spill trajectory modeling primarily concentrated on parameter combinations, including a current drift coefficient, a wind drag coefficient, and a wave-induced Stokes drift coefficient (Cucco et al., 2012; Tian et al., 2017; Yang et al., 2023; Yu et al., 2017). While this integral and relatively coarse calibration approach could result in satisfactory model results, quantifying and revealing the individual effects of parameters, especially turbulent diffusion, remained unclear. Thus, a separate calibration of individual parameters, such as diffusion coefficients, is strongly needed.

In terms of model performance evaluation, previous studies typically employed visual comparisons, such as satellite images and coastal reports, and a separation index to assess discrepancies between simulated and observed trajectories (Chen, 2021; Cucco et al., 2012; De Dominicis et al., 2016; French-McCay et al., 2017; Tian et al., 2017). While these methods are valid to some extent, many of them focus on a single aspect, such as either the separation distance or the overlap area. Such metrics may not offer a comprehensive understanding of the fundamental nature of particle movement, including directional and length aspects. Consequently, our insight into which aspect is more critical for accurately simulating particle movement may be limited. This gap in knowledge impedes the identification of specific areas for model performance enhancement, hindering the efficient utilization of the model.

In this study, we focused on Lake Erie, where the spill risk is increasing and model calibration and evaluation are strongly needed for emergency response, while observational data is seriously lacking (Song et al., 2024). We drove the GNOME model (an LPM) using the lake surface current data derived from the experimental version of the Great Lakes Operational Forecast System (GLOFS). In addition, we utilized three Coastal Ocean Dynamics Experiment (CODE) drifters to obtain their trajectory data. The aim is to (1) propose a practical and simple convex hull calibration method using drifter data to determine the optimal diffusion coefficients for the daily application of the GNOME model, (2) evaluate the model performance by defining two performance metrics, namely direction and length indicators, in addition to using the well-known separation index. These results help form a simple method to calibrate LPMs, providing a scientific basis for future model applications and emergency oil spill response.

## 2. Materials and Methods

### 2.1 Study area and drifter data

Lake Erie, one of the North American Great Lakes, was selected as the focal study and observation site for calibrating the GNOME model in this study. Covering a surface area of approximately 25,700 square kilometers, with a maximum depth of about 64 meters and an average depth of around 19 meters (Fig. 1A), Lake Erie is a vital economic hub for shipping, fishing, and recreation (Arnillas et al., 2020). Notably, it hosts major ports such as those in the cities of Toledo and Cleveland, Ohio, supporting a flourishing commercial shipping industry. Due to its economic significance and the need for efficient emergency response to oil spill events, as well as the imperative to safeguard the water environment, we leveraged three drifter trajectories to calibrate the particle diffusion process in the GNOME model in this study (Fig. 1B-D). These trajectories represent the most comprehensive drifter data for Lake Erie available from 2011 onward (see Supplementary Material).

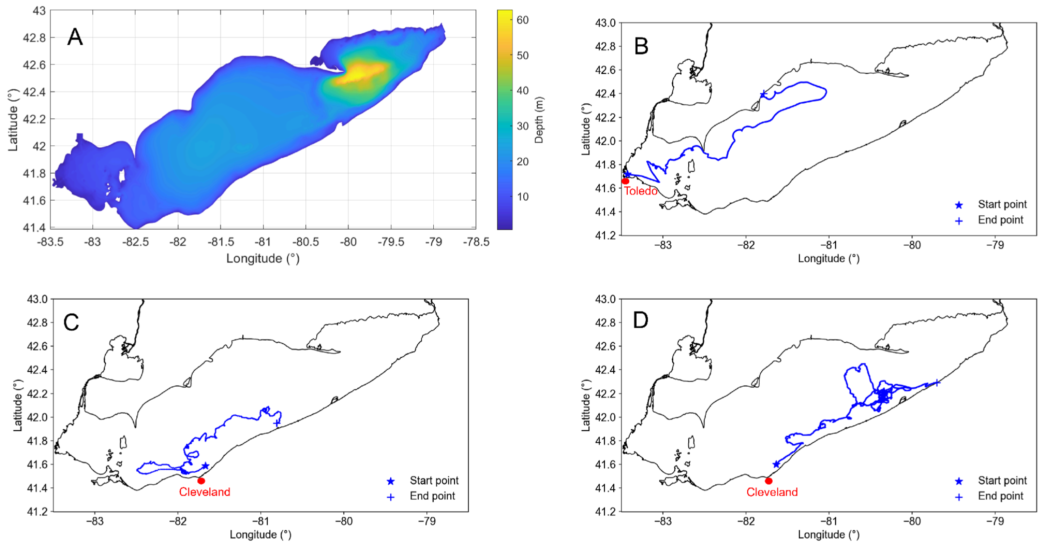


**Fig. 1.** (A) Bathymetry map of Lake Erie, (B) Drifter trajectory from July 5, 2016 to August 5, 2016, (C) Drifter trajectory from August 31, 2018 to October 25, 2018, (D) Drifter trajectory from September 13, 2019 to December 17, 2019.

One drifter was deployed on the water surface in the nearshore region of Toledo, recording its location data from July 5, 2016, to August 5, 2016, during which it was not stranded on the shoreline (Fig. 1 B). The other two drifters were deployed at the water surface in the nearshore region of Cleveland (Fig. 1C-D). The first drifter was released on August 31, 2018, recording its location data until October 25, 2018 (Fig. 1C). The second drifter was deployed from September 13 to December 17, 2019 (Fig. 1D). The GPS location, including latitude and longitude, of the drifter was recorded hourly. It is important to highlight that the CODE drifters used in this study were comprised of a 1-meter-long vertical tube with four wings, remaining fully submerged to minimize the impact of wind. In the simulation of drifter trajectories, the wind module was turned off based on the drifter design, and currents served as the sole driving force in the GNOME model to propel particles.

## 2.2 GNOME model

### 2.2.1 Model description

This study utilized the GNOME model, with its computational core being PyGNOME, a 3-D particle tracking computational codebase developed by the NOAA Office of Response and Restoration, Emergency Response Division (MacFadyen and Barker, 2024). The GNOME model is based on the Lagrangian particle tracking method for simulating the transport process of oil particles in water environments (Akinbamini Oluyemi et al., 2022; Balogun et al., 2021). The main equation used for simulating particle transport is described as follows.

$$\vec{L}_{t_0+\Delta t} = \vec{L}_{t_0} + \int_{t_0}^{t_0+\Delta t} \vec{V}[x(t),\ y(t),\ t]dt \tag{1}$$

where $\vec{L}_{t_0+\Delta t}$ is the new position of an oil particle at the moment of $t_0 + \Delta t$, $\vec{L}_{t_0}$ is the original position of the oil particle at the moment of $t_0$, $\vec{V}[x(t),\ y(t),\ t]$ is the velocity of the oil particle at the time $t$ and the location $(x(t),\ y(t))$. The particle movement in the GNOME model relies on the simple linear superposition of currents, winds, and diffusion (Barker et al., 2023).

The sub-grid scale circulations are represented using a random walk diffusion algorithm (Barker et al., 2023). Meanwhile, the GNOME model relies entirely on external forcings such as currents and wind. Herein, we used the hydrodynamic output mainly including lake surface current data from the experimental version of the Great Lakes Operational Forecast System (GLOFS) to drive the GNOME model. The GLOFS has been well-validated for water level, water temperature, heat flux, and ice concentration in our previous research (Anderson et al., 2018; Fujisaki-Manome et al., 2020), though validation of currents has not been conducted, largely due to a lack of observational current data against which to validate the model results.

In this study, we calculated the time derivatives of the drifter horizontal positions to estimate currents at different locations and times in Lake Erie (Fig. S1) (Choi et al., 2020; Smith et al., 2023). This approach allowed us, for the first time, to validate the GLOFS-simulated currents, demonstrating that the model can reliably reproduce currents (Fig. S1). However, discrepancies were observed, possibly due to spatial discretization errors within the model and the use of averaged currents from the estimation method instead of actual instantaneous currents at specific points (Fig. S1) (Smith et al., 2023).

#### 2.2.2 Model setup

As the actual drifter is designed to remain unaffected by the wind and is driven by the current, we did not include the wind process in the particle trajectory simulation within the GNOME model (De Dominicis et al., 2016; Song et al., 2024). Notably, a single released particle will realize only one of many possible trajectories from the initial location, even if the diffusion parameterization is perfect in the model (Csanady, 2012). Therefore, to calibrate the diffusion coefficient, we released 1000 particles (default number in the model) at the initial location of the drifter trajectory and compared the observed drifter trajectory with the trajectory of the position center of all particles (particle cloud). The driving currents from GLOFS remain constant across simulation scenarios that share the same simulation period but have different diffusion coefficients. In this scenario, the diffusion coefficient within a random walk algorithm (isotropic and constant over time and space), which represents the horizontal diffusion of particles due to small-scale circulations like eddies not captured in the model, becomes the sole parameter driving the separation of particle trajectories (Barker et al., 2023).

Additionally, to minimize deviations between the released particles and the drifter and to maintain their correlation, we set the simulation period to one day, consistent with the short-term predictions used in emergency response applications (Montas et al., 2020; Xu et al., 2013). The calculation time step is set as 30 min. To efficiently utilize the drifter data, we established the starting points for particle simulations along the observed drifter trajectory, with a restarting time interval of 12 hours. As a result, there are a total of 62 cases from July 5, 2016, to August 5, 2016; 110 cases from August 31, 2018, to October 25, 2018; and 190 cases from September 13, 2019, to December 17, 2019.

### 2.3 Convex hull method for calibrating diffusion coefficients

The convex hull of a set of points is defined as the smallest convex polygon that surrounds all the points in the set (Barber et al., 1996). Building upon this, we have established a criterion: in a specific 1-day drifter simulation scenario, if the convex hull formed by the trajectories of 1000 simulated particles encompasses the observed drifter trajectories, we consider the GNOME model trajectory under the corresponding diffusion coefficient to be valid to capture the observed drifter trajectories (Fig. 2) (Rowe et al., 2022). Consequently, running each 1-day scenario for a range of diffusion coefficients (1-200 $m^2$ $s^{-1}$, at intervals of 2) to determine the smallest diffusion coefficient (*SDC*) that ensures the inclusion of observed drifter trajectories within the convex hull of the simulated particles represents a simple and viable strategy to reduce over-diffusion errors and determine the optimal diffusion coefficient (Fig. 2). Over-diffusion errors occur when the diffusion coefficient is determined to be high, causing simulated particles to spread far and resulting in large convex polygons that easily include observed drifter trajectories. This endeavor stands as the primary objective in the calibration of diffusion coefficients. The derivation of a convex hull was based on the *scipy.spatial.ConvexHull* of the SciPy library with Python.

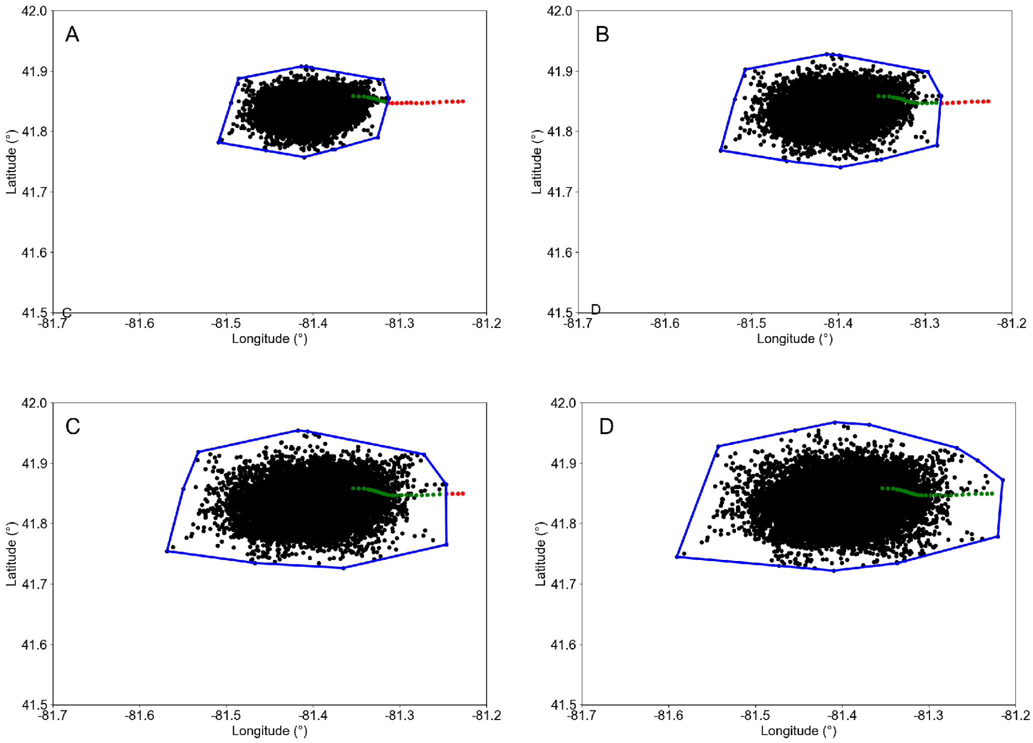


**Fig. 2.** An example of using the convex hull method and different diffusion coefficients to find the smallest diffusion coefficient for one drifter trajectory: (A) 30 $m^2$ $s^{-1}$, (B) 50 $m^2$ $s^{-1}$, (C) 80 $m^2$ $s^{-1}$, (D) 100 $m^2$ $s^{-1}$. Black dots represent the trajectories of simulated particles during the 1-day simulation period. Green dots represent a portion of the drifter trajectory enclosed within the convex hull polygon. Red dots represent a portion of the drifter trajectory outside the convex hull polygon. If all drifter trajectories are within the convex hull polygon, it is considered that the corresponding diffusion coefficient makes the model capture the observed drifter trajectory.

### 2.4 Direction and length indicators for analyzing model performance

In this study, we have established non-dimensional indicators for both direction and length, facilitating a more direct and comprehensive analysis of the model performance (Fig. 3).

$$DI = \cos cos\, \theta \tag{2}$$

$$LI = \frac{1}{1+|(SL-OL)/OL|} \tag{3}$$

where $DI$ is the direction indicator, θ is the angle between the observed vector of the drifter (beginning at the initial trajectory point and ending at the final trajectory point) and the simulated vector of the particle cloud (beginning at the initial trajectory point and ending at the average/centroid location of particles at the end of their movement), $LI$ is the length indicator, $SL$ is the length of the simulated vector of the particle cloud, $OL$ is the length of the observed vector of the drifter. For both *DI* and *LI*, the best score is 1, and the worst score is -1 for *DL* and approaches 0 for *LI*.

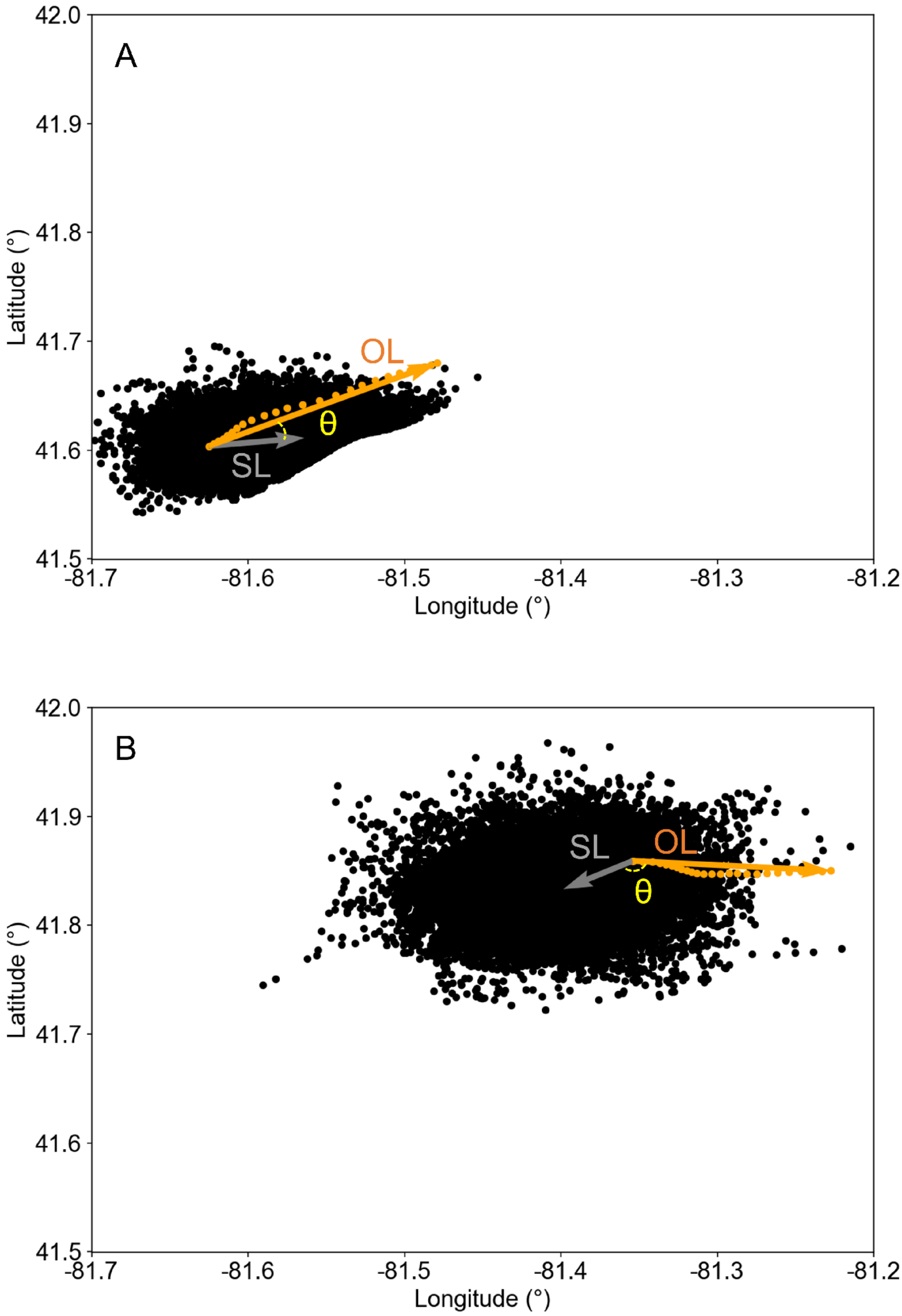


**Fig. 3.** Conceptual illustration of the indicators for assessing the model performance: (A) The simulated particle cloud moves in the same direction with the drifter trajectory, (B) The simulated particle cloud moves in the opposite direction to the drifter trajectory. Black dots represent simulated particles. Orange dots represent drifter trajectories. The grey vector

represents the simulated vector of the particle cloud. The orange vector represents the observed vector of the drifter.

### 2.5 Separation index for analyzing model performance

We used the dimensionless traditional separation index (*SI*) skill score for comparison with the proposed indicators and further revelation of the model performance (Fig. S2) (French-McCay et al., 2017; Liu and Weisberg, 2011). The separation index characterizes the discrepancy between simulated and observed trajectories and is defined as follows.

$$SI = \frac{\sum_{i=1}^{N} d_i}{\sum_{i=1}^{N} O_i} \tag{4}$$

Where $SI$ is the separation index, $i$ is the time step of 1 hour, $N$ is the number of the time steps, $O_i$ is the accumulated length of the observed trajectory at time step $i$, $d_i (\geq 0)$ is the separation distance between the location of the observed drifter and the average location of the simulated particles at time step $i$. *SI* has a minimum value of 0 (perfect match) or larger. If the *SI* is larger than 1.0, it means that the separation distance is greater than the magnitude of the observed drifter movement, indicating that the model has "no skill" (Dearden et al., 2022).

### 2.6 Statistical analysis

To capture the potential mechanisms and relationships between *SDC*, *DI*, *LI*, and *SI*, Spearman correlation analysis was employed in this study. This non-parametric measure is ideal for assessing the strength and direction of monotonic relationships between two variables because it does not assume normality or linearity, making it effective for analyzing variables that may not meet these assumptions. The thresholds were defined based on the p-values: a p-value less than 0.05 ($^*$) was considered significant, and a p-value less than 0.01 ($^{**}$) was considered highly significant. In addition, histograms, which are graphical representations that organize a group of data points into a specified range, were also utilized in this study for a more comprehensive understanding of data distribution.

## 3. Results

### 3.1 *SDC*

Based on the proposed convex hull method, we calibrated the GNOME model for 362 one-day observed drifter trajectories by determining the corresponding *SDC*s. 314 out of 362 obtained *SDC*s range from 2 $m^2\ s^{-1}$ to 22 $m^2\ s^{-1}$ (Fig. 4). In addition, the average *SDC* and the median *SDC* for all 362 cases are 14 $m^2\ s^{-1}$ and 8 $m^2\ s^{-1}$, respectively. Subsequently, we visualized the spatial distribution of *SDC*s by placing and gridding the *SDC* values at the initial location where the drifters started their trajectories for 62 cases in 2016, 110 cases in 2018 and 190 cases in 2019 (Fig. 5 and Fig. S3). 7 out of 362 cases had *SDC*s greater than 100 $m^2\ s^{-1}$, all of which occurred in 2016 due to missing meteorological data and the use of an older version of GLOFS, leading to lower accuracy in the simulated driving currents (Fig. 5 and Fig. S3).

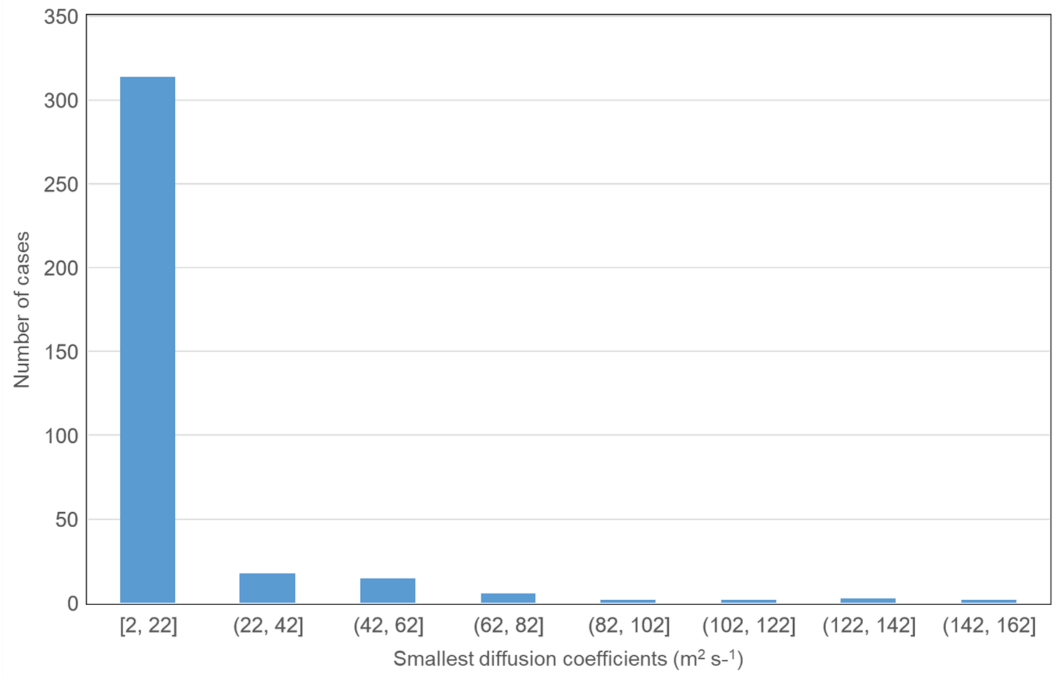


**Fig. 4.** Bar chart illustrating the distribution of the *SDC*s across 362 simulation cases. The *SDC*s are grouped into intervals of 20 $m^2$ $s^{-1}$, with the majority of cases falling within the lowest interval range of 2 to 22 $m^2$ $s^{-1}$.

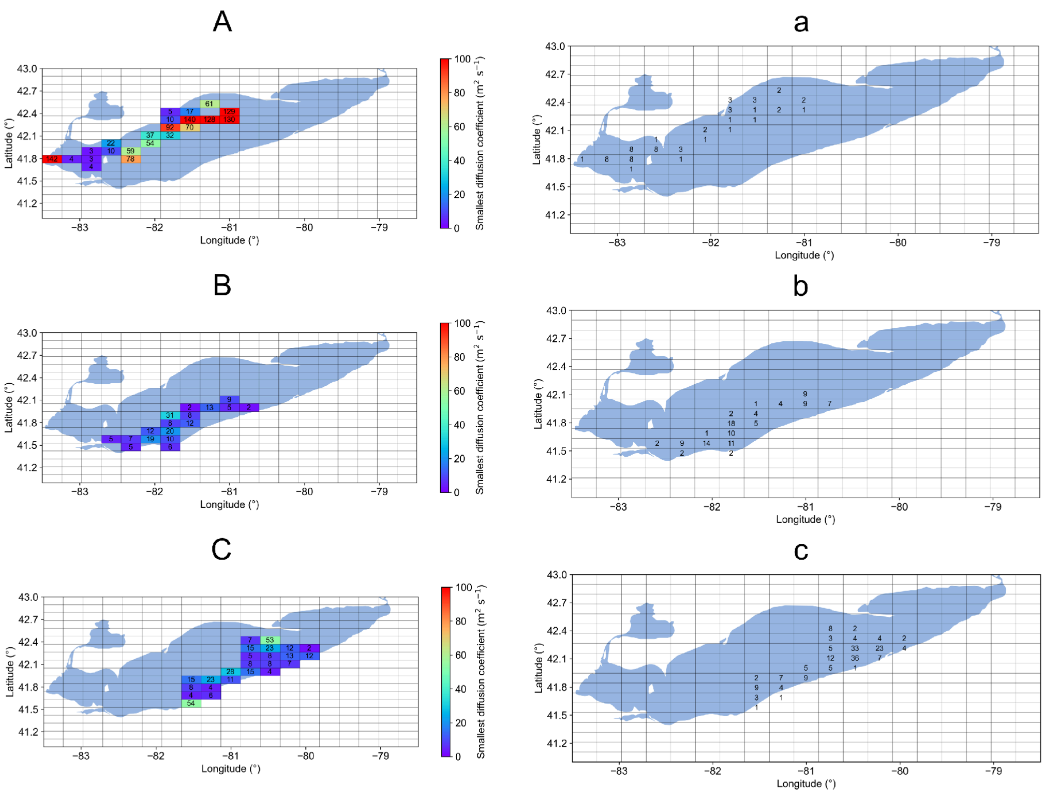

**Fig. 5.** Spatial distribution of the gridded average *SDC*s: (A) for 2016, (B) for 2018, (C) for 2019. The numbers in each grid represent the average *SDC* of the corresponding region. The number of cases in each grid used for calculating the average *SDC*: (a) for 2016, (b) for 2018, (c) for 2019.

### 3.2 *DI* and *LI*

To evaluate the model performance, we calculated both the direction and length indicators for 362 one-day cases. For the directional simulation of particle movement, 267 out of 362 cases demonstrate a *DI* value within the range of 0.7-1.0 (Fig. 6A), This range corresponds to the angle between the observed vector of the drifter and the simulated vector of the particle cloud being 0°-45.6°. These results suggest that the model performed relatively well in replicating the direction of particle movement. In addition, 186 out of 362 cases exhibit an *LI* value smaller than 0.7 (Fig. 6B), indicating discrepancies between *SL* and *OL*.

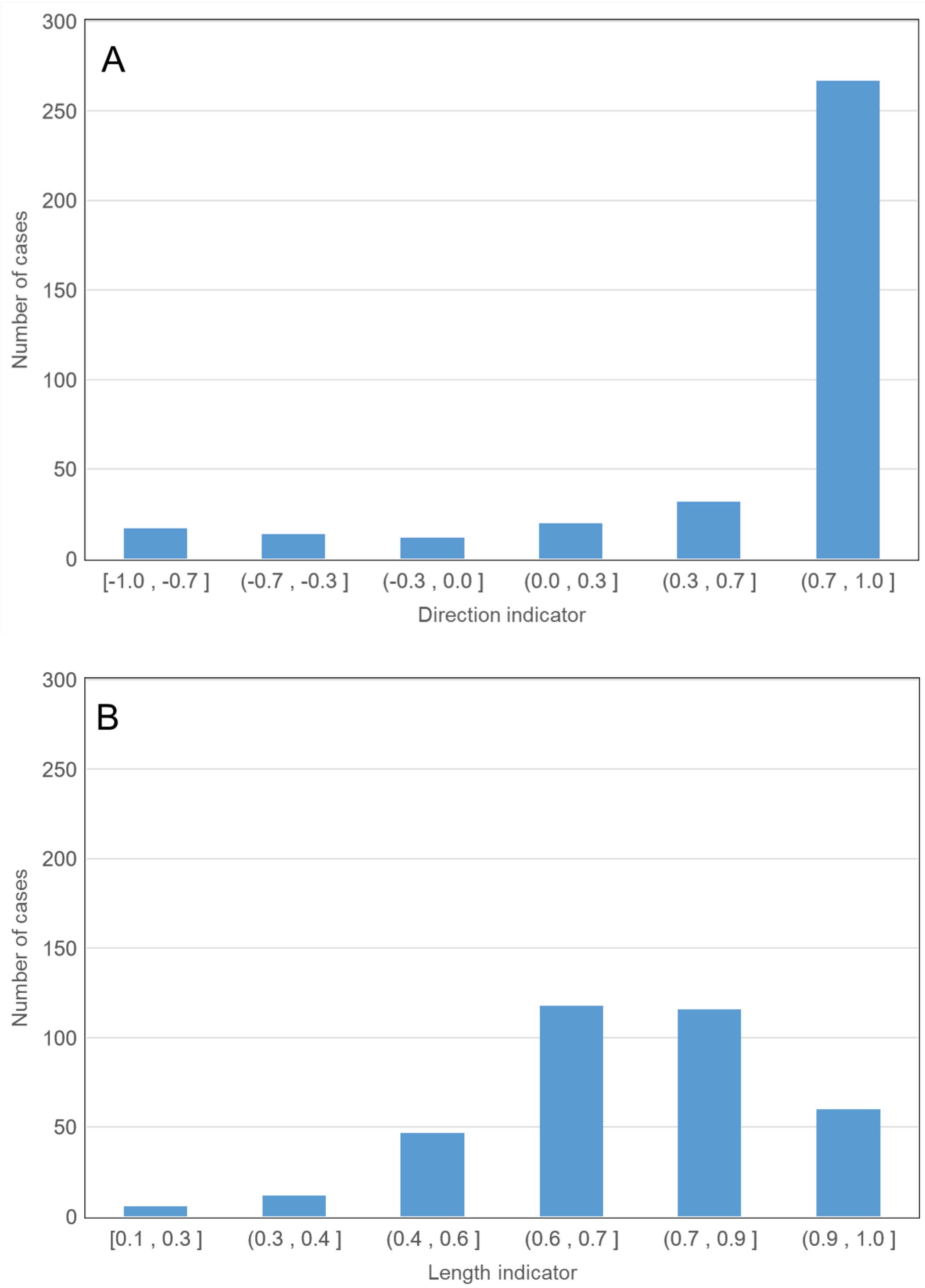


**Fig. 6.** Bar charts illustrating the distributions of the two proposed indicators across 362 simulation cases: (A) *DI*, (B) *LI*.

### 3.3 *SI*

For a comprehensive evaluation of the calibrated model, we computed the introduced *SI* for all 362 one-day cases. In 302 out of 362 cases, the *SI* values fall within the interval of 0-1.0 (Fig. 7), indicating that the accumulated separation distance is shorter than the accumulated length of the observed drifter trajectory. For the remaining 60 cases, the *SI* values are greater than 1, suggesting the model has 'no skill' because the separation distance exceeds that of the observed drifter trajectory.

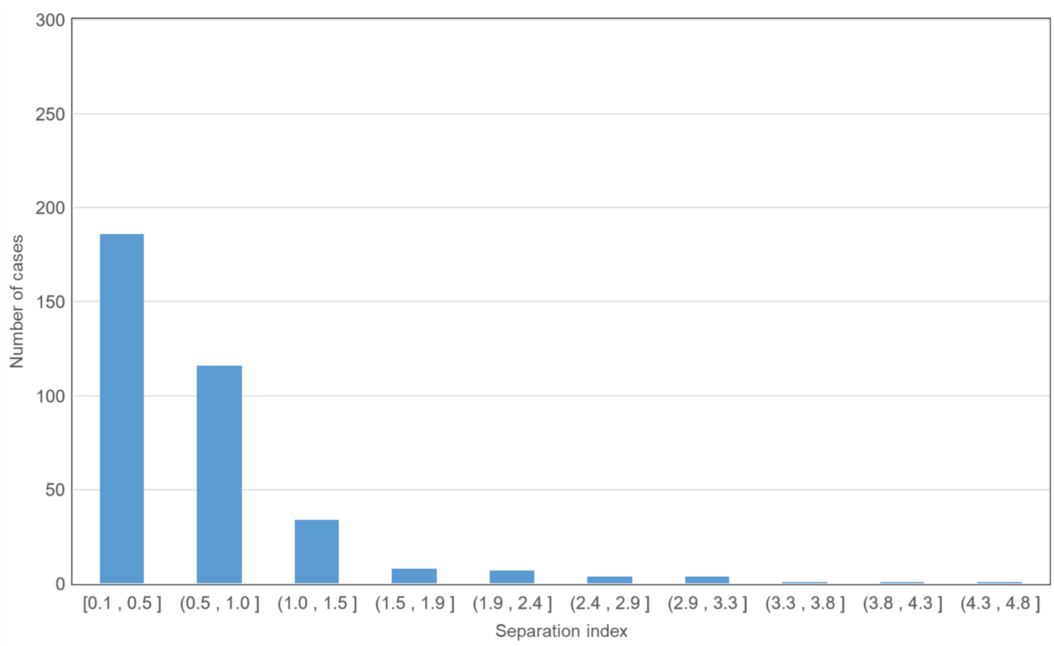


**Fig. 7.** Bar chart illustrating the distribution of the *SI* across 362 simulation cases.

## 4. Discussion

### 4.1 Significance of the convex hull method

In this study, we examined the convex hull method to calibrate the diffusion coefficient in the GNOME model. The convex hull method was used to identify the smallest envelope of the simulated particle cloud, covering all drifter trajectory dots. Notably, this concise method emphasizes the overall shape and distribution alignment between simulated and observed trajectories. To some extent, the method proves more efficient when contrasted with approaches that rely on intricate mathematical equations to minimize separation distance or depend on post-processing satellite images (Abascal et al., 2009; Tian et al., 2017; Yang et al., 2023). The method also facilitates the efficient utilization of precise and high-temporal-resolution (i.e., hourly) drifter data for calibrating LPMs, especially in areas lacking observational oil trajectory data (Dearden et al., 2022). Collectively, the convex hull method provides a simple way to calibrate diffusion coefficients in LPMs, making them well-prepared for simulating particle trajectories, especially in the case of emergency oil spills.

Nevertheless, the method may fall short in accounting for specific drifter trajectories, leading to a lack of resolution/accuracy in capturing the intricacies of particle movements, such as individual random trajectories. Given our objective to calibrate the diffusion process of spilled particles, characterized by substantial irregularity and stochasticity, the focus should remain on the spatial distribution or shape of the particles, while detailed internal discrepancies may not be a primary consideration.

### 4.2 Comparison of the calibrated diffusion coefficient with other estimates

Utilizing the proposed convex hull method, we calibrated the diffusion coefficient in the GNOME model by determining *SDC* to mitigate potential over-diffusion errors. The average *SDC* from 362 one-day cases in 2016, 2018, and 2019 is 14 $m^2$ $s^{-1}$, suggesting a recommended diffusion coefficient for predicting particle trajectories in Lake Erie using the GNOME model. This value closely aligns with reported diffusion coefficient values (10-20 $m^2$ $s^{-1}$) recommended for marine environments, demonstrating the effectiveness of the proposed convex hull calibration method (Abascal et al., 2017; Gurumoorthi et al., 2021; Matsuzaki and Fujita, 2014).

Moreover, the value is also close to, and probably more accurate than, the average value 212 $m^2$ $s^{-1}$ (ranging from 27 $m^2$ $s^{-1}$ to 399 $m^2$ $s^{-1}$) for Lake Erie, which was obtained from a mesh-size-based empirical equation in previous studies ($diffusion\, coefficient = 0.03 \times mesh\, size^{1.15}$) (de Brauwere et al., 2011; Rowe et al., 2022), further validating the reliability of the convex hull method. Therefore, 14 $m^2$ $s^{-1}$ is determined to be the optimal diffusion coefficient for simulating particle trajectories in Lake Erie.

On the other hand, previous studies have reported that optimal diffusion coefficients can vary, ranging from areas outside the continental slope to those over the continental slope and shelf, and are also highly dependent on the input datasets (Abascal et al., 2009; Tian et al., 2017). Given that the recommended diffusion coefficient of 14 $m^2$ $s^{-1}$ is derived from the confined space of the drifter trajectory, extending the coverage area of drifter deployment would be helpful for improving robustness. A potential limitation of the convex hull method is its sensitivity to outlier particles, which may occur due to strong horizontal shear in the currents. However, no obvious outliers were observed during the simulations in this study, possibly becasue of the short 1-day simulation period. Future research on this limitation may be needed. If an outlier is identified, we need to proceed with caution in interpreting the results. Specifically, we could assess whether the outlier enables the convex hull formed by the released particles to easily encompass the trajectory points of the drifter. If this is the case, the estimated *SDC* may be smaller than the true value.

### 4.3 Assessing the model performance using *DI*, *LI*, and *SI*

To assess the model performance in reproducing the desired characteristics (direction and length) of the observed drifter trajectories using the convex hull method, we defined two indicators, *DI* and *LI*. The two indicators provide a comprehensive and direct understanding of the fundamental nature of the overall movement of the particle cloud, including directional and length aspects, rather than the separation distance or overlap area (French-McCay et al., 2017; Yang et al., 2023). Among the 362 cases, 267 demonstrate a *DI* value greater than 0.7 (Fig. 6A), underscoring the calibrated model's proficiency in capturing the direction of drifter movement. Note that the convex hull method primarily focuses on determining the smallest diffusion coefficients to ensure the coverage of released particles over drifter trajectories. This approach has minimal impact on the overall direction of the released particle cloud, which is primarily influenced by the currents (De Dominicis et al., 2013). Furthermore, when the moving direction of the released particle cloud aligns closely with the drifter trajectory, the smallest diffusion coefficient tends to be smaller, consistent with the negative and significant relationship between *DI* with *SDC* ($r$ = -0.34, $P < 0.01$, Fig. S4). This is because the error in simulated currents from GLOFS could be small and there is less requirement to substantially increase the diffusion effect to ensure the released particle cloud covers the drifter trajectories.

Regarding *LI*, more than half of the values below 0.7 implies that the calibrated model has errors in predicting *OL*. More deeply, in 247 out of 362 cases, *SL* is smaller than *OL*. This phenomenon could be attributed to the inaccuracy in the lake surface current data, which is the main driving force for drifter movement (Barker et al., 2023). Moreover, *LI* demonstrates a negative and significant relationship with *SDC* ($r$ = -0.41, $P < 0.01$, Fig. S4), suggesting that a more accurate simulation of particle travel distance associated with small errors in currents leads to a decrease in diffusion when matching the simulated particle cloud with the drifter trajectory. It is important to note that biases in simulated currents, such as being weaker than actual values or moving in the opposite direction of actual vectors, can result in large *SDC* values that may not accurately represent sub-grid scale diffusion in the GNOME model.

Additionally, we introduced *SI* to quantify the degree of discrepancy between the simulated particle trajectory and the observed drifter trajectory, providing a comprehensive assessment of the calibrated model using the convex hull method. The majority of cases (302 out of 362) show an *SI* value smaller than 1.0, indicating that the smallest diffusion coefficients, calibrated by the convex hull method, effectively ensure the model's performance, maintaining a reasonable range for the discrepancy between simulated and observed trajectories compared to previous studies (Cucco et al., 2012; De Dominicis et al., 2016; French-McCay et al., 2017). The positive and significant relationship between *SDC* and *SI* suggests that a smaller *SDC* value with less potential over-diffusion may inhibit the separation distance ($r = 0.45$, $P < 0.01$, Fig. S4). Furthermore, both *DI* and *LI* exhibit significant and negative correlations with *SI* ($r = -0.50$ and $-0.53$, respectively, $P < 0.01$, Fig. S4) while the correlation between *DI* and *LI* is weak ($r = 0.16$, $P < 0.01$, Fig. S4). This indicates that the accuracy in predicting both aspects (overall direction of particle cloud movement and travel length) plays a key role in determining the model performance.

In practice, we can first use *SI* as a comprehensive indicator to evaluate the model performance because the model must perform well in both directional and length aspects (both *DI* and *LI* must be higher) to result in a lower *SI*. If we have a higher *SI*, we can further investigate *DI* and *LI* to identify which aspect(s) weakens the model performance.

### 4.4. Limitations

While the convex hull method has proven to be efficient for calibrating the diffusion coefficient based on limited drifter data, this study has some limitations.

First, the recommended diffusion coefficient of 14 $m^2$ $s^{-1}$ is derived from three available drifter trajectories in a confined space, which may affect accuracy and representativeness. This limitation is due to the lack of observational data in Lake Erie. Second, it is worth noting that when the simulated and observed trajectories do not match, there are two potential reasons: sub-grid scale diffusion and error in the external currents. In this study, we used drifter trajectories to estimate actual currents and validated the external current measurements, despite the presence of estimation approximations. Due to the absence of observational current data in Lake Erie, it is challenging to accurately quantify current errors and even more difficult to distinguish their effect from diffusion. Therefore, the calibration relies on the input currents being utilized. This dependence could make the optimal diffusion coefficient more tailored to the input currents and accelerate the calibration process. However, this also means that the calibrated diffusion process accounts for both sub-grid scale movements and errors in the predicted currents. For a more accurate calibration process, it is beneficial to deploy current measurement tools to collect spatial current data for driving the GNOME model. This approach could be more accurate than using predicted currents from GLOFS to drive the GNOME model.

## 5. Conclusions

To calibrate LPMs in the absence of available observational data in water bodies, we proposed the simple convex hull method and utilized drifter trajectories to determine optimal diffusion coefficients for the implementation of the GNOME model in Lake Erie. Moreover, we defined *DI* and *LI* and introduced *SI* to assess the model performance. The main findings are as follows.

(1) Even with the trajectory data of a single drifter, the convex hull method proved to be an efficient approach for calibrating the diffusion process in LPMs, making them well-prepared for emergency use in simulating particle trajectories.

(2) The recommended diffusion coefficient of 14 $m^2 s^{-1}$ for GNOME model use in Lake Erie aligns closely with the values suggested for marine environments and those calculated through previous empirical methods, validating the reliability of the convex hull method.

(3) The calibrated model with *SDC*s showcased the capability to accurately replicate the movement direction of drifters and efficiently manage the disparity between simulated and observed trajectories, thereby preventing over-diffusion. Both the directional aspect and length aspect were found to be crucial for accurately simulating particle movements.

(4) The calibrated model exhibited a tendency to underpredict the travel distance of drifters. This limitation could stem from the errors in the driving force, namely, current data. Higher predicting accuracies, particularly in direction and length (corresponding to higher *DI* and *LI*), likely indicate small errors in currents from GLOFS, thus leading to a decrease in *SDC*.

In summary, the proposed convex hull method offers a simple approach to utilizing drifter trajectories for calibrating diffusion coefficients in LPMs. The defined *DI* and *LI* reveal more in-depth information about model performance. These results support using LPMs to simulate particle trajectories and enhance emergency response. For future research, gathering additional observational data, such as oil spill trajectory and current data, could further explore the diffusion process and test the convex hull method.

## Acknowledgments

This work was supported by the U.S. Coast Guard Great Lakes Oil Spill Center of Expertise awarded to the National Oceanic and Atmospheric Administration (NOAA) and the Cooperative Institute for Great Lakes Research (CIGLR) through the NOAA Cooperative Agreement with the University of Michigan (NA17OAR4320152). This is a GLERL contribution XXXX and CIGLR contribution XXXX. The Authors would like to thank Lacey Mason, Matt Alloy, Nancy E. Kinner, and Kathy Mandsager for their part in making this work possible.

# CRediT authorship contribution statement

**Yang Song**: Conceptualization, Methodology, Writing - original draft, Investigation, Formal analysis, Visualization, Software, Validation, Data curation, Writing - review & editing.

**Ayumi Fujisaki-Manome**: Validation, Software, Funding acquisition, Writing - review & editing.

**Christopher H. Barker**: Conceptualization, Methodology, Software, Writing - review & editing.

**Amy MacFadyen**: Validation, Software, Writing - review & editing.

**Dan Titze**: Formal analysis, Validation, Writing - review & editing.

**James Kessler**: Software, Writing - review & editing.

**Jia Wang**: Writing - review & editing.

## References


1 Abascal, A.J., Castanedo, S., Mendez, F.J., Medina, R., Losada, I.J., 2009. Calibration of a Lagrangian Transport Model Using Drifting Buoys Deployed during the "Prestige" Oil Spill. Journal of Coastal Research 25(1), 80-149.

2 Abascal, A.J., Castanedo, S., Núñez, P., Mellor, A., Clements, A., Pérez, B., Cárdenas, M., Chiri, H., Medina, R., 2017. A high-resolution operational forecast system for oil spill response in Belfast Lough. Marine Pollution Bulletin 114(1), 302-314.

3 Akinbamini Oluyemi, E., Anifowose, B., Obioma Eric, C., 2022. Oil Spill Modeling for the Mariner Oil Field, East of Shetland, United Kingdom, North Sea. Journal of Environmental Engineering 148(8), 04022037.

4 Albeldawi, M., 2023. Chapter 10 - Environmental impacts and mitigation measures of offshore oil and gas activities, in: Hussein, I.A., Mahmoud, M. (Eds.), Developments in Petroleum Science. Elsevier, pp. 313-352.

5 Anderson, E.J., Fujisaki-Manome, A., Kessler, J., Lang, G.A., Chu, P.Y., Kelley, J.G.W., Chen, Y., Wang, J., 2018. Ice Forecasting in the Next-Generation Great Lakes Operational Forecast System (GLOFS), Journal of Marine Science and Engineering. p. 123.

6 Arnillas, C.A., Yang, C., Zamaria, S.A., Neumann, A., Javed, A., Shimoda, Y., Feisthauer, N., Crolla, A., Dong, F., Blukacz-Richards, A., Rao, Y.R., Paredes, D., Arhonditsis, G.B., 2020. Integrating watershed and ecosystem service models to assess best management practice efficiency: guidelines for Lake Erie managers and watershed modellers. Environmental Reviews 29(1), 31-63.

7 Balogun, A.-L., Yekeen, S.T., Pradhan, B., Wan Yusof, K.B., 2021. Oil spill trajectory modelling and environmental vulnerability mapping using GNOME model and GIS. Environmental Pollution 268, 115812.

8 Barber, C.B., Dobkin, D.P., Huhdanpaa, H., 1996. The quickhull algorithm for convex hulls. ACM Trans. Math. Softw. 22(4), 469–483.

9 Barker, C.H., Jones, R., Lehr, W.J., MacFadyen, A., O'Connor, C., Makela, J., Hennen, J., 2023. GNOME Technical Documentation (Draft). NOAA Office of Response and Restoration. Seattle, WA.

10 Barker, C.H., Kourafalou, V.H., Beegle-Krause, C.J., Boufadel, M., Bourassa, M.A., Buschang, S.G., Androulidakis, Y., Chassignet, E.P., Dagestad, K.-F., Danmeier, D.G., Dissanayake, A.L., Galt, J.A., Jacobs, G., Marcotte, G., Özgökmen, T., Pinardi, N., Schiller, R.V., Socolofsky, S.A., Thrift-Viveros, D., Zelenke, B., Zhang, A., Zheng, Y., 2020. Progress in Operational Modeling in Support of Oil Spill Response, Journal of Marine Science and Engineering. p. 668.

11 Bhattacharjee, S., Dutta, T., 2022. Chapter 1 - An overview of oil pollution and oil-spilling incidents, in: Das, P., Manna, S., Pandey, J.K. (Eds.), Advances in Oil-Water Separation. Elsevier, pp. 3-15.

12 Cakir, E., Sevgili, C., Fiskin, R., 2021. An analysis of severity of oil spill caused by vessel accidents. Transportation Research Part D: Transport and Environment 90, 102662.

13 Chen, J., Zhang, W., Wan, Z., Li, S., Huang, T., Fei, Y., 2019. Oil spills from global tankers: Status review and future governance. Journal of Cleaner Production 227, 20-32.

14 Chen, Y., 2021. Development of an oil spill model adaptable to exposure and submergence conversion of tidal flats: A case study in the Changjiang Estuary. Marine Pollution Bulletin 171, 112715.

15 Choi, J., Troy, C., Hawley, N., McCormick, M., Wells, M., 2020. Lateral dispersion of dye and drifters in the center of a very large lake. Limnology and Oceanography 65(2), 336-348.

16 Csanady, G.T., 2012. Turbulent diffusion in the environment. Springer Science & Business Media.

17 Cucco, A., Sinerchia, M., Ribotti, A., Olita, A., Fazioli, L., Perilli, A., Sorgente, B., Borghini, M., Schroeder, K., Sorgente, R., 2012. A high-resolution real-time forecasting system for predicting the fate of oil spills in the Strait of Bonifacio (western Mediterranean Sea). Marine Pollution Bulletin 64(6), 1186-1200.

18 Dagestad, K.F., Röhrs, J., Breivik, Ø., Ådlandsvik, B., 2018. OpenDrift v1.0: a generic framework for trajectory modelling. Geosci. Model Dev. 11(4), 1405-1420.

19 de Brauwere, A., de Brye, B., Servais, P., Passerat, J., Deleersnijder, E., 2011. Modelling Escherichia coli concentrations in the tidal Scheldt river and estuary. Water Research 45(9), 2724-2738.

20 De Dominicis, M., Bruciaferri, D., Gerin, R., Pinardi, N., Poulain, P.M., Garreau, P., Zodiatis, G., Perivoliotis, L., Fazioli, L., Sorgente, R., Manganiello, C., 2016. A multi-model assessment of the impact of currents, waves and wind in modelling surface drifters and oil spill. Deep Sea Research Part II: Topical Studies in Oceanography 133, 21-38.

21 De Dominicis, M., Pinardi, N., Zodiatis, G., Archetti, R., 2013. MEDSLIK-II, a Lagrangian marine surface oil spill model for short-term forecasting – Part 2: Numerical simulations and validations. Geosci. Model Dev. 6(6), 1871-1888.

22 Dearden, C., Culmer, T., Brooke, R., 2022. Performance Measures for Validation of Oil Spill Dispersion Models Based on Satellite and Coastal Data. IEEE Journal of Oceanic Engineering 47(1), 126-140.

23 Dong, C.-D., Nguyen, T.-H.-H., Hou, T.-H., Tsai, C.-C., 2019. Integrated numerical model for the simulation of the ts taipei oil spill. Journal of Marine Science and Technology 27(4), 7.

24 French-McCay, D.P., Tajalli-Bakhsh, T., Jayko, K., Spaulding, M.L., Li, Z., 2017. Validation of oil spill transport and fate modeling in Arctic ice. Arctic Science 4(1), 71-97.

25 Fujisaki-Manome, A., Mann, G.E., Anderson, E.J., Chu, P.Y., Fitzpatrick, L.E., Benjamin, S.G., James, E.P., Smirnova, T.G., Alexander, C.R., Wright, D.M., 2020. Improvements to Lake-Effect Snow Forecasts Using a One-Way Air–Lake Model Coupling Approach. Journal of Hydrometeorology 21(12), 2813-2828.

26 Goeury, C., Hervouet, J.-M., Baudin-Bizien, I., Thouvenel, F., 2014. A Lagrangian/Eulerian oil spill model for continental waters. Journal of Hydraulic Research 52(1), 36-48.

27 Guo, W., Jiang, M., Li, X., Ren, B., 2018. Using a genetic algorithm to improve oil spill prediction. Marine Pollution Bulletin 135, 386-396.

28 Gurumoorthi, K., Suneel, V., Trinadha Rao, V., Thomas, A.P., Alex, M.J., 2021. Fate of MV Wakashio oil spill off Mauritius coast through modelling and remote sensing observations. Marine Pollution Bulletin 172, 112892.

29 Ivanov, L.M., Collins, C.A., Margolina, T., 2021. Reconstruction of Diffusion Coefficients and Power Exponents from Single Lagrangian Trajectories. Fluids 6(3), 111.

30 Jiang, P., Tong, S., Wang, Y., Xu, G., 2021. Modelling the oil spill transport in inland waterways based on experimental study. Environmental Pollution 284, 117473.

31 Johnston, J.E., Lim, E., Roh, H., 2019. Impact of upstream oil extraction and environmental public health: A review of the evidence. Science of the Total Environment 657, 187-199.

32 Keramea, P., Spanoudaki, K., Zodiatis, G., Gikas, G., Sylaios, G., 2021. Oil Spill Modeling: A Critical Review on Current Trends, Perspectives, and Challenges. Journal of Marine Science and Engineering 9(2), 181.

33 Li, P., Cai, Q., Lin, W., Chen, B., Zhang, B., 2016. Offshore oil spill response practices and emerging challenges. Marine Pollution Bulletin 110(1), 6-27.

34 Liu, Y., Weisberg, R.H., 2011. Evaluation of trajectory modeling in different dynamic regions using normalized cumulative Lagrangian separation. Journal of Geophysical Research: Oceans 116(C9).

35 MacFadyen, A., Barker, C.H., 2024. NOAA's Response Modeling – Challenges and Innovations, International Oil Spill Conference Proceedings. In press.

36 Matsuzaki, Y., Fujita, I., 2014. Horizontal turbulent diffusion at sea surface for oil transport simulation. Coastal Engineering Proceedings 1(34), management.8.

37 Montas, L., Ferguson, A.C., Mena, K.D., Solo-Gabriele, H.M., 2020. Categorization of nearshore sampling data using oil slick trajectory predictions. Marine Pollution Bulletin 150, 110577.

38 Nordam, T., Beegle-Krause, C.J., Skancke, J., Nepstad, R., Reed, M., 2019. Improving oil spill trajectory modelling in the Arctic. Marine Pollution Bulletin 140, 65-74.

39 Rowe, M.D., Prendergast, S.E., Alofs, K.M., Bunnell, D.B., Rutherford, E.S., Anderson, E.J., 2022. Predicting larval alewife transport in Lake Michigan using hydrodynamic and Lagrangian particle dispersion models. Limnology and Oceanography 67(9), 2042-2058.

40 Smith, S.R., Helber, R.W., Jacobs, G.A., Barron, C.N., Carrier, M., Rowley, C., Ngodock, H., Pasmans, I., Bartels, B., DeHaan, C., Yaremchuk, M., 2023. Ocean drifter velocity data assimilation Part 2: Forecast validation. Ocean Modelling 185, 102260.

41 Song, Y., Fujisaki-Manome, A., Barker, C.H., MacFadyen, A., Kessler, J., Titze, D., Wang, J., 2024. Modeling study on oil spill transport in the Great Lakes: The unignorable impact of ice cover. Journal of Environmental Management 358, 120810.

42 Tian, S., Huang, X., Li, H., 2017. A new method to calibrate Lagrangian model with ASAR images for oil slick trajectory. Marine Pollution Bulletin 116(1), 95-102.

43 Xu, H.-L., Chen, J.-N., Wang, S.-D., Liu, Y., 2012. Oil spill forecast model based on uncertainty analysis: A case study of Dalian Oil Spill. Ocean Engineering 54, 206-212.

44 Xu, Q., Li, X., Wei, Y., Tang, Z., Cheng, Y., Pichel, W.G., 2013. Satellite observations and modeling of oil spill trajectories in the Bohai Sea. Marine Pollution Bulletin 71(1), 107-116.

45 Yang, Z., Chen, Z., Lee, K., 2023. Development and testing of a 2D offshore oil spill modeling tool (OSMT) supported by an effective calibration method. Marine Pollution Bulletin 188, 114696.

46 Yu, F., Li, J., Zhao, Y., Li, Q., Chen, G., 2017. Calibration of backward-in-time model using drifting buoys in the East China Sea. Oceanologia 59(3), 238-247.

# Supplementary information

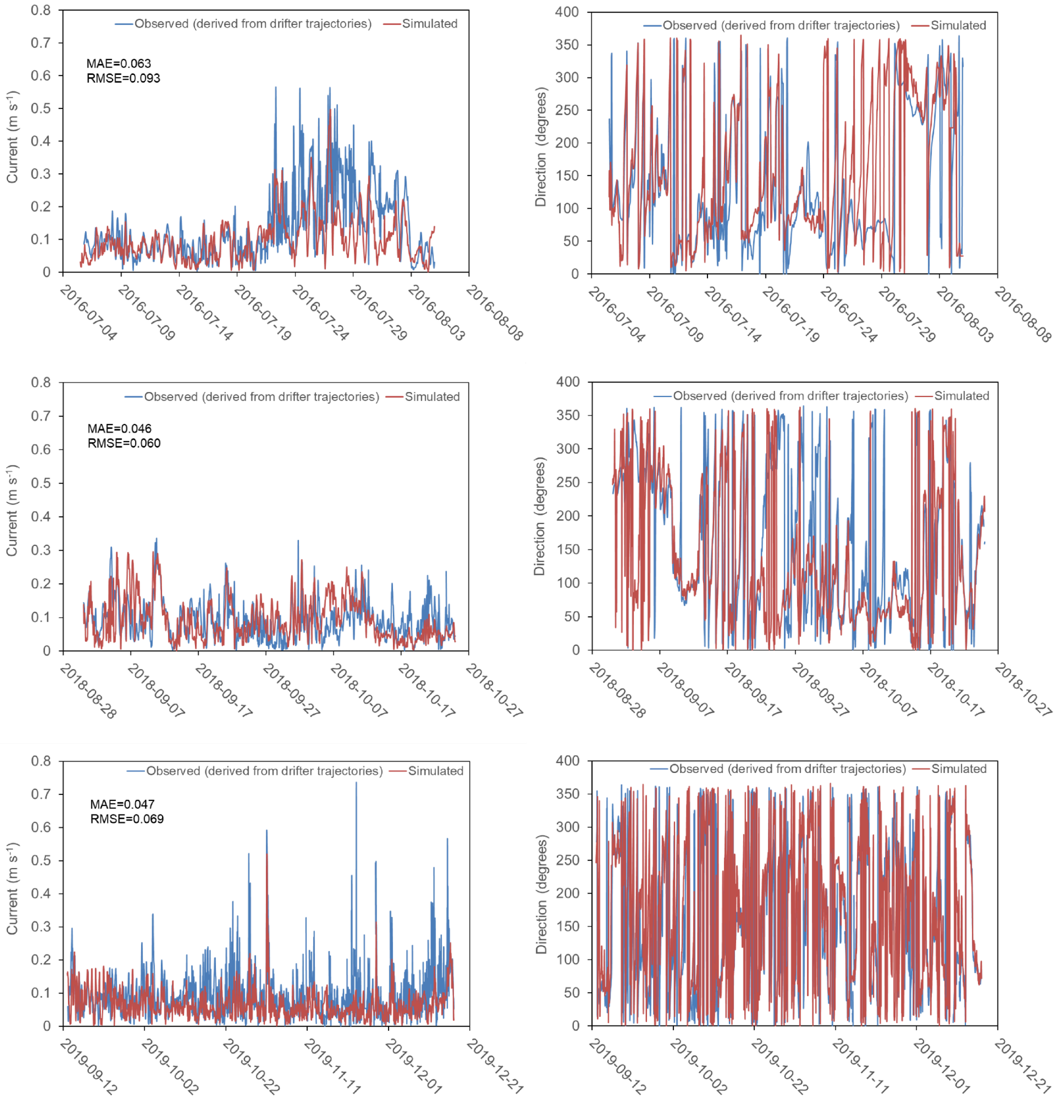


**Fig. S1.** Validation of simulated currents from the GLOFS model using observed drifter trajectories. MAE indicates the mean absolute error, and RMSE indicates the root mean square error. Note that 0 degrees represents North, and angles increase clockwise.

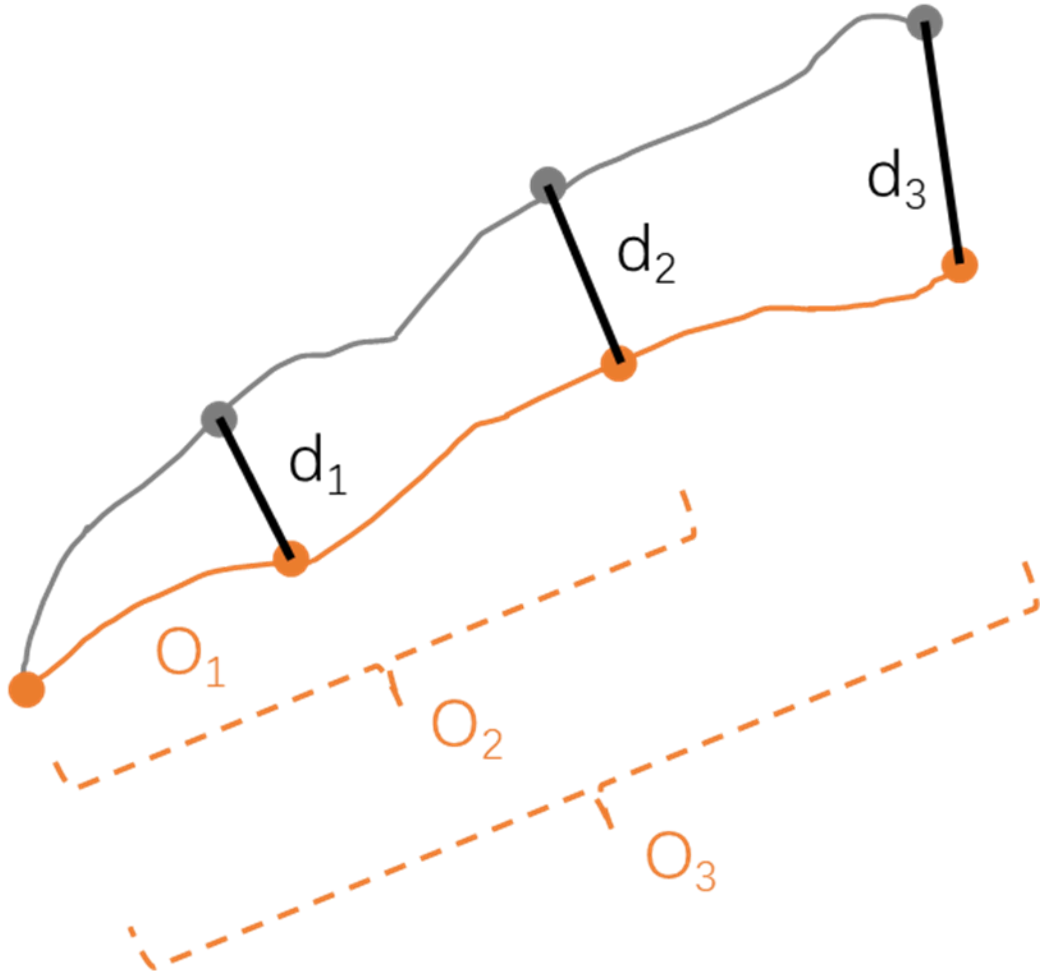


**Fig. S2.** Conceptual illustration of *SI*. The grey dot represents the average location of simulated particles and the orange dot represents the drifter trajectories. $O_i$ is the accumulated length of the actual observed trajectory and $d_i$ is the separation distance.

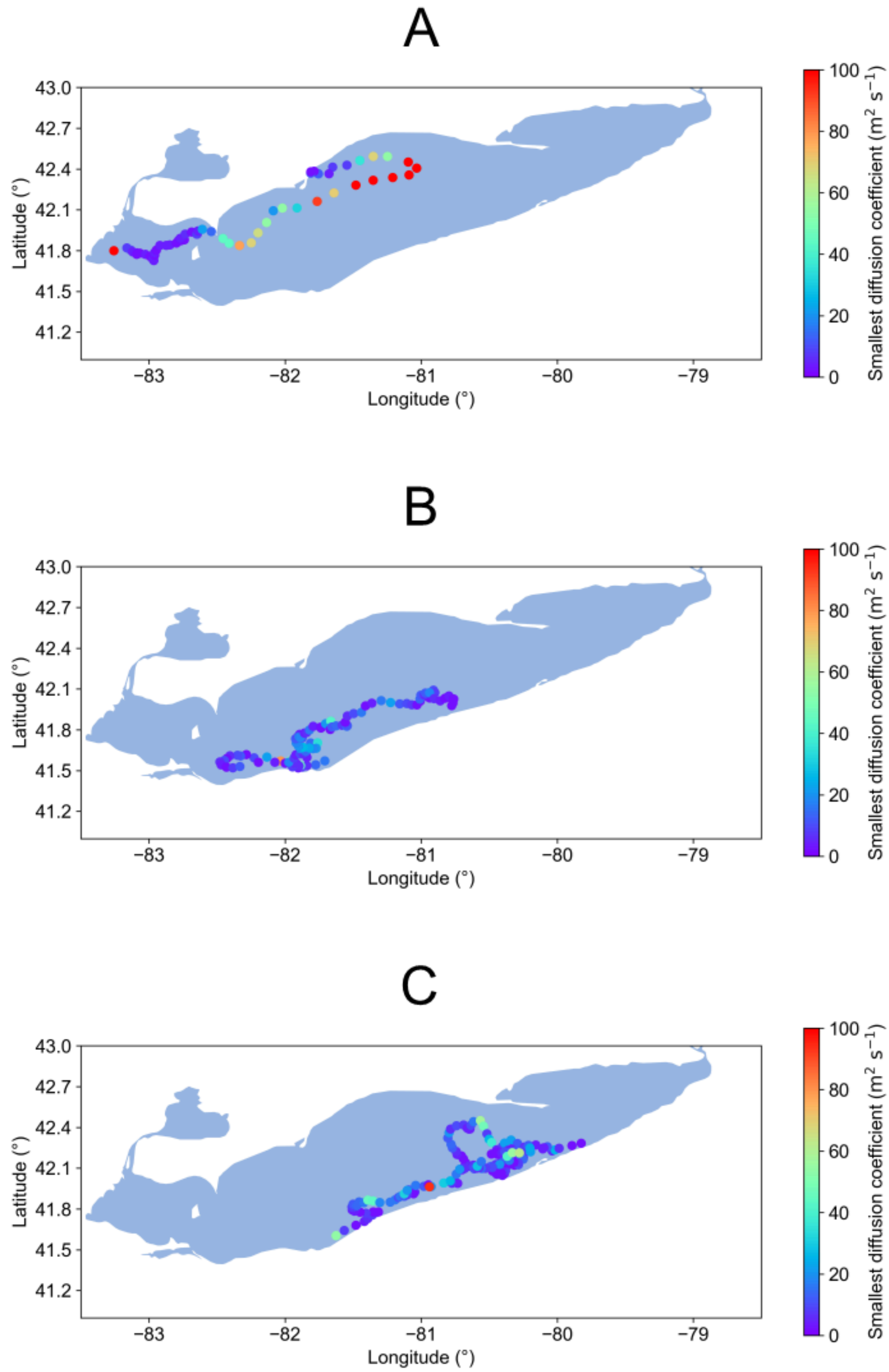


**Fig. S3.** Spatial distribution of the *SDC*s: (A) 62 cases in 2016, (B) 110 cases in 2018, (C) 190 cases in 2019.

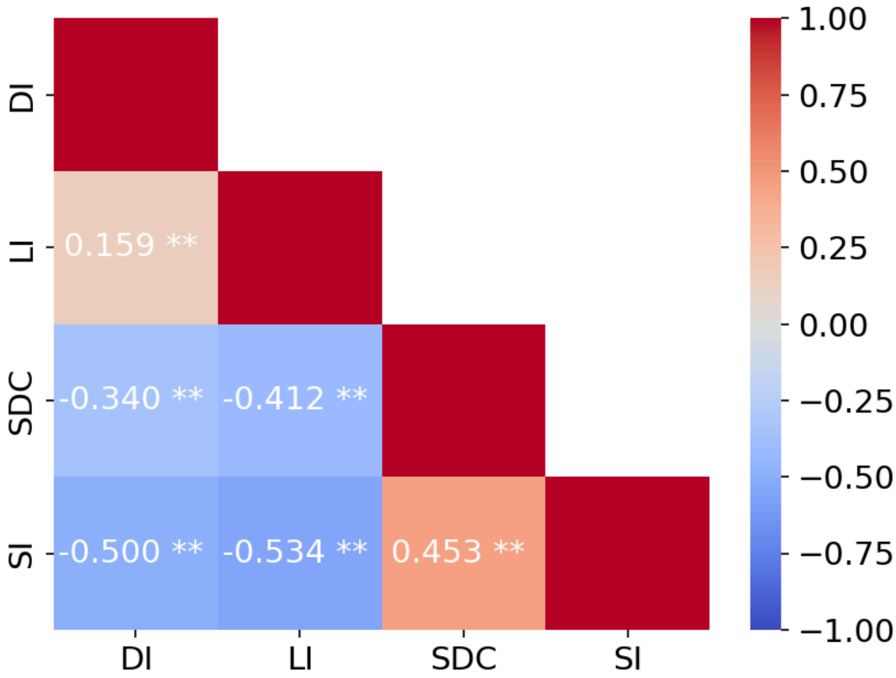


**Fig. S4.** Spearman correlations for *DI*, *LI*, *SDC*, and *SI*. * indicates $P < 0.05$, and ** indicates $P < 0.01$.